

Energy Bands in Iron via the Augmented Plane Wave Method*

J. H. WOOD

Solid-State and Molecular Theory Group, Massachusetts Institute of Technology, Cambridge, Massachusetts

(Received November 27, 1961)

Results of numerical calculations of the band structure of body-centered cubic and face-centered cubic iron are reported; the calculations have been carried out according to the augmented plane wave (APW) method of Slater. A total of 55 points in the $1/48$ of the Brillouin zone has been examined in the bcc case; this provides sufficient information for construction of a density-of-states curve which is presented. For the fcc structure, calculations have been performed at 17 points of high symmetry; no density-of-states curve is calculated.

The potential used is that of Manning and consists of the argon core plus 7 valence electrons. The lattice constants are taken as

$a=3.647 \times 10^{-8}$ cm for the fcc lattice and $a=2.861 \times 10^{-8}$ cm for the bcc lattice. Fortunately, the latter constant is one of the three used by Stern in a modified tight-binding calculation of the cohesive energy and band structure of iron. Rather good agreement is found between the present calculation and Stern's.

The APW method seems a promising one inasmuch as the convergence in terms of number of plane waves is reached in about 40 plane waves (this for a point in the Brillouin zone having *no* symmetry). Moreover, the method is one which is quite adaptable to a digital computer and has been programmed for the Whirlwind computer (by Saffren) and for the IBM 704 and 709 computers.

INTRODUCTION

THE energy bands of solids have long been of interest although it has been only in recent years, with the advent of the large scale digital computer, that it has proved possible to obtain solutions to this problem in which one can have confidence and so assess the limits of validity of the one-electron approach. Reviews of the energy band formalism and the results (both early and postwar) have been given by Slater, Reitz, and Callaway.¹⁻³

Here, we report on calculations of the energy band structure of body-centered cubic and face-centered cubic iron. As in the other band calculations on iron, these calculations take no direct account of the magnetization; thus, the one-electron potential is taken to be independent of the spin-orientation of the electron for whose wave function we are solving. The calculations were carried out using the augmented plane wave (APW) method developed by Slater in 1937.⁴

The APW method was first applied to copper by Chodorow.⁵ A variant of the method, due to Saffren and Slater,⁶ was used by Howarth in a calculation on copper.⁷ At the time of Howarth's work it appeared that the earlier version was one which could not be accommodated on a computer of the size then available. Later work by Saffren⁸ proved this assumption false and he

then set up this 1937-APW method on the MIT Whirlwind computer. The author subsequently adapted the method to the IBM 704 and 709 computers, where, of course, size is no longer a problem. Calculations performed by Burdick⁹ on copper with the restrictions Chodorow assumed in his calculation give results identical to Chodorow's. Moreover, excellent agreement (to 5 figures) exists among the Whirlwind and 704-709 results.

The work on iron was initiated on Whirlwind, using Saffren's programs. The particular choice of iron was made because of general interest in the transition metals and also in order to determine the usefulness of the APW method in a problem involving $3d$ electrons where we might expect convergence difficulties.

THE APW METHOD

The theory of the 1937 augmented plane wave method has been developed by Slater.⁴ The motivating assumption of the method is that the crystal potential for a valence electron in a metal can be chosen to have the "muffin-tin" form. That is, around each nucleus of the lattice one takes an appropriate spherically symmetric potential, delimited by a sphere of radius R_s . In the region between such spheres, one chooses the potential to be constant. This potential is now the one used in the one-electron Schrödinger equation and this together with the imposition of the usual periodic boundary conditions determines, in principle, the solutions of the problem. In view of the choice of potential, one now expands the unknown one-electron wave functions in terms of a particular set of trial functions ψ_i consisting of plane waves in the constant potential region and a general spherical solution inside the spheres. If we choose a single plane wave $e^{i\mathbf{k}\cdot\mathbf{r}}$ in the region of constant potential, then the other portion of this trial function (around the sphere at location r_n)

* Part of a thesis submitted in partial fulfillment of the requirements for the PhD degree in Physics at the Massachusetts Institute of Technology. This work was supported in part by the Office of Naval Research, and in part by the U. S. Army, Navy, and Air Force.

¹ J. C. Slater, *Handbuch der Physik*, edited by S. Flügge (Springer-Verlag, Berlin, 1956), Vol. XIX, p. 1.

² J. R. Reitz, *Solid-State Physics*, edited by F. Seitz and D. Turnbull (Academic Press, Inc., New York, 1955), Vol. 1, p. 1.

³ J. Callaway, *Solid-State Physics*, edited by F. Seitz and D. Turnbull (Academic Press, Inc., New York, 1958), Vol. 7, p. 100.

⁴ J. C. Slater, *Phys. Rev.* **51**, 846 (1937).

⁵ M. I. Chodorow, Ph.D. thesis, Department of Physics, Massachusetts Institute of Technology, 1939 (unpublished); *Phys. Rev.* **55**, 675 (1939).

⁶ M. M. Saffren and J. C. Slater, *Phys. Rev.* **92**, 1126 (1953).

⁷ D. J. Howarth, *Phys. Rev.* **99**, 469 (1955).

⁸ M. M. Saffren, *Bull. Am. Phys. Soc.* **5**, 298 (1960). See also M. M. Saffren, *ibid.* **5**, 281 (1960).

⁹ G. A. Burdick, Ph.D. thesis, Department of Physics, Massachusetts Institute of Technology, 1961 (unpublished); *Phys. Rev. Letters* **7**, 156 (1961).

will be⁴

$$\begin{aligned} \psi_i = \exp(i\mathbf{k} \cdot \mathbf{r}_n) \sum_{l=0}^{\infty} \sum_{m=-l}^{+l} (2l+1) i^l \frac{j_l(kR_n)}{u_l(R_n; E)} \\ \times u_l(|\mathbf{r}-\mathbf{r}_n|; E) \frac{(l-|m|)!}{(l+|m|)!} P_l^{|m|}(\cos\theta) \\ \times P_l^{|m|}(\cos\theta') \exp[im(\phi-\phi')]. \end{aligned}$$

θ' and ϕ' refer to the direction of \mathbf{k} where we take the origin of the coordinate system at \mathbf{r}_n . The j_l are spherical Bessel functions. Here, the coefficients in the spherical expansion are so chosen that the plane-wave portion matches on continuously in *value* to this expansion. The $u_l(r; E)$ are solutions of the radial wave equation

$$-\frac{1}{r^2} \frac{d}{dr} \left(r^2 \frac{du_l}{dr} \right) + \left(\frac{l(l+1)}{r^2} + V(r) \right) u_l = E u_l, \quad (1)$$

where $V(r)$ is the spherically symmetric potential. Such a function consisting of the plane wave plus the spherical solution is referred to as an augmented plane wave (APW); the solution of the energy band problem can then be regarded as one of determining the coefficients for the expansion of the true one-electron wave function $\Psi_k(\mathbf{r})$ in terms of a set of APW's, ψ_i ,

$$\Psi_k(\mathbf{r}) = \sum_i v_i \psi_i.$$

The index i on ψ_i is a multiple index; each APW is k dependent through its plane-wave portion and carries an implicit energy dependence through the $u_l(r; E)$ appearing in the spherical sum. The solution of the energy band problem

$$H\Psi_k = E\Psi_k, \quad (2)$$

in terms of APW's is then resolved into the solution of a secular equation. This is, we must find the zeroes of $\det\{(H-E)_{ij}\}$, where $(H-E)$ is the matrix whose elements are

$$(H-E)_{ij} = \int \psi_i^*(H-E)\psi_j d\tau. \quad (3)$$

Thus, the energy appears in the nondiagonal terms both explicitly, and implicitly by way of the radial solutions. The entire determinant is a complicated function of the energy; numerical evaluation of this determinant as a function of the energy allows one to determine the zeroes in energy and thus the approximate eigenvalues of the problem.

The form of $(H-E)_{ij}$ is given by Slater⁴ for one atom per unit cell as

$$(H-E)_{ij} = (\mathbf{k}_i \cdot \mathbf{k}_j - E)\delta_{ij} + (1/\Omega)F_{ij},$$

where

$$\begin{aligned} F_{ij} = 4\pi R_s^2 \left[-(\mathbf{k}_i \cdot \mathbf{k}_j - E) \frac{j_1(|\mathbf{k}_j - \mathbf{k}_i| R_s)}{|\mathbf{k}_j - \mathbf{k}_i|} \right. \\ \left. + \sum_{l=0}^{\infty} (2l+1) P_l(\cos\theta_{ij}) j_l(k_i R_s) j_l(k_j R_s) \right. \\ \left. \times \frac{u_l'(R_s; E)}{u_l(R_s; E)} \right]. \quad (4) \end{aligned}$$

Here Ω is the volume of the unit cell, R_s is the radius of the sphere, the j_l 's are spherical Bessel functions, the P_l 's are Legendre polynomials, and the u_l 's are the solutions of Eq. (1) for the energy E .

METHOD OF COMPUTATION

Having selected a point \mathbf{k} in the first Brillouin zone at which we wish to solve Eq. (2), we must now select the APW's ψ_i from which the matrix of $(H-E)$ is to be constructed.

First we take account of Bloch's theorem which tells us that the wave vector \mathbf{k}_i to be associated with ψ_i is drawn from the set $\{\mathbf{k} + \mathbf{K}_i\}$, the \mathbf{K}_i being the infinite set of the reciprocal lattice vectors. Furthermore, for reasons which will be discussed, it was desirable to initially restrict this set such that no member could be obtained from some other member by an operation of the group of the wave vector¹⁰ \mathbf{k} . Computer programs were written to generate this reduced set of $\{\mathbf{k} + \mathbf{K}_i\}$ for the bcc and fcc lattices; the Whirlwind programs being written by Saffren⁸ and IBM programs by the author.

Next, in order to conserve computation time, it is useful to take account of the general result that Ψ_k and the ψ_i APW's out of which it is composed, must transform according to one of the irreducible representations of the group of the wave vector.¹⁰ This can be accomplished by the use of group projection operators¹¹; employing these operators permits one to obtain all the functions (derived from the various ψ_i) which transform according to a chosen irreducible representation. From the α th irreducible representation of dimension n_α one can form n_α^2 projection operators ρ_{ij}^α . These have the general form¹¹ (for a unitary representation)

$$\rho_{ij}^\alpha = \sum_R \Gamma_\alpha(R)_{ij}^* R. \quad (5)$$

$\Gamma_\alpha(R)_{ij}^*$ is the complex conjugate of the ij matrix element in the matrix representing the operation R in the α th irreducible representation and the sum is over all the operations R in the group. One may apply such a projection operator to any function f and obtain a new

¹⁰ L. P. Bouckaert, R. Smoluchowski, and E. Wigner, Phys. Rev. **50**, 58 (1936).

¹¹ G. F. Koster, Technical Report No. 8, Solid State and Molecular Theory Group, Massachusetts Institute of Technology, 1956 (unpublished); V. Heine, *Group Theory in Quantum Mechanics* (Pergamon Press, New York, 1960).

function f_{ij}^α :

$$\rho_{ij}^\alpha f = f_{ij}^\alpha. \quad (6)$$

f_{ij}^α now will have definite transformation properties under the group and in particular if R is any operation in the group.¹¹

$$Rf_{ij}^\alpha = \sum_k \Gamma_\alpha(R)_{ki} f_{kj}^\alpha. \quad (7)$$

Thus all such symmetrized functions, derived from f , which bear the same second index transform among themselves and are, in fact, partners in a basis for this α th irreducible representation. The transformation coefficients for any one of these partners f_{ij}^α are taken from the i th column of the matrix $\Gamma_\alpha(R)$.

Now if f and g are any two functions and O is an operator which transforms according to the identity representation of the group, then the following holds true (G is the order of the group and n_α is the dimensionality of the α th irreducible representation):

$$\langle \rho_{ij}^\alpha f | O | \rho_{kl}^\beta g \rangle = (G/n_\alpha) \delta_{\alpha\beta} \delta_{ik} \langle f | O | \rho_{jl}^\alpha g \rangle, \quad (8)$$

so that there are no matrix elements between partners in the same irreducible representation and no elements between different irreducible representations. Furthermore, the value of the matrix element (8) is the same for all rows so that one need solve only the secular equation among basis functions transforming according to the same column in the irreducible representation. The n_α identical solutions of the secular equation merely reflect the degeneracy of the problem—as the first index of the projection operators is changed, we obtain the n_α partners defined by our eigenvectors.

If f and g are taken to be APW's ψ_i and ψ_j and O is the operator $(H-E)$, then we have the relation (to within a constant):

$$(H-E)_{ij}^\alpha = \sum_R \frac{G}{n_\alpha} [\Gamma_{jil}(R)]^* \langle \psi_i | H-E | R\psi_j \rangle,$$

where

$$\begin{aligned} \langle \psi_i | H-E | R\psi_j \rangle &= (\mathbf{k}_i \cdot R\mathbf{k}_j - E) \\ &\times [\Omega \delta_{ij} - 4\pi R_s^2 j_1(|R\mathbf{k}_j - \mathbf{k}_i| R_s) / |R\mathbf{k}_j - \mathbf{k}_i|] \\ &+ 4\pi R_s^2 \sum_{l=0}^{\infty} (2l+1) P_l \left(\frac{\mathbf{k}_i \cdot R\mathbf{k}_j}{|\mathbf{k}_i| |\mathbf{k}_j|} \right) \\ &\times j_l(k_i R_s) j_l(k_j R_s) \frac{u_l'(R_s; E)}{u_l(R_s; E)}. \quad (10) \end{aligned}$$

Computer programs for automatically forming the matrix elements (10) have been written for Whirlwind by Saffern⁸ and for the IBM machines by the author.¹² The \mathbf{k}_i and \mathbf{k}_j occurring here are members of the previously mentioned reduced set $\{\mathbf{k} + \mathbf{K}_i\}$ appropriate to

TABLE I. Listing of one-electron potential in rydberg units used in calculations reported here. Values of r are in atomic units. In the bcc case this potential is cut off at radius 2.341 and the constant potential between spheres is taken at 0.816 ry. In the fcc case, cutoff is taken at radius 2.437 and the constant is taken as 0.776 ry. These constants are spherical averages of the tabulated potential between the inscribed spheres of the above radii and the Wigner-Seitz spheres, the latter having the radii 2.662 for the bcc case and 2.693 for the fcc case.

r	$V(r)$	r	$V(r)$
0.005	10173.0	0.840	10.30
0.010	4977.5	0.880	9.240
0.015	3247.3	0.920	8.322
0.020	2384.6	0.960	7.523
0.025	1870.0	1.000	6.824
0.030	1528.1	1.040	6.211
0.035	1285.3	1.080	5.669
0.040	1104.4	1.120	5.193
0.045	964.53	1.160	4.773
0.050	853.28	1.200	4.400
0.055	762.80	1.240	4.068
0.060	687.83	1.280	3.770
0.065	624.78	1.320	3.501
0.070	571.06	1.360	3.258
0.075	524.72	1.400	3.039
0.080	484.40	1.440	2.839
0.085	448.96	1.480	2.657
0.090	417.66	1.520	2.492
0.095	389.78	1.560	2.341
0.100	364.82	1.600	2.202
		1.640	2.075
0.110	322.02	1.680	1.958
0.120	286.74	1.720	1.850
0.130	257.24	1.760	1.750
0.140	232.24	1.800	1.658
0.150	210.87	1.840	1.573
0.160	192.46	1.880	1.494
0.170	176.44	1.920	1.421
0.180	162.37	1.960	1.354
0.190	150.01	2.000	1.292
0.200	139.12	2.040	1.234
		2.080	1.181
0.220	121.29	2.120	1.132
0.240	106.02	2.160	1.086
0.260	93.642	2.200	1.045
0.280	83.582	2.240	1.006
0.300	75.023	2.280	0.9715
0.320	67.741	2.320	0.9392
		2.360	0.9093
0.360	55.986	2.400	0.8812
0.400	46.915	2.440	0.8545
0.440	39.716	2.480	0.8277
0.480	33.890	2.520	0.8032
0.520	29.112	2.560	0.7783
0.560	25.146	2.600	0.7558
0.600	21.835	2.640	0.7347
0.640	19.048	2.680	0.7135
0.680	16.697	2.720	0.6932
0.720	14.701	2.760	0.6736
0.760	13.00	2.800	0.6546
0.800	11.54	2.840	0.6362

the particular \mathbf{k} . We see here the reason for using the reduced set—all other members are now automatically generated by the operations R forming the group of k . The input to the programs consists of specification of the irreducible representation α , a list of wave vectors $\{\mathbf{k} + \mathbf{K}_i\}$ for a particular point \mathbf{k} , and along with each wave vector the appropriate (second) projection operator index. In addition, one includes a list of energies E for which the determinant of the matrix $(H-E)_{ij}$ is

¹² J. H. Wood, Quarterly Progress Report No. 36, Solid State and Molecular Theory Group, Massachusetts Institute of Technology, 1960 (unpublished).

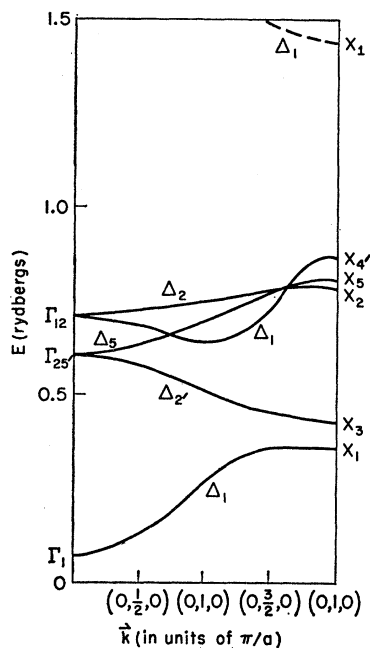


FIG. 1. Energy bands in fcc iron from $\Gamma(0,0,0)$ to $X(0,2,0)$ along $[010]$ direction.

to be evaluated. Determination of the group of the wave vector [which determines the set R to be used in Eq. (10)], formation of the quantities $u_i'(R_s)/u_i(R_s)$ from the spherical portion of the potential for each energy and generation of the Bessel and Legendre functions then proceeds automatically, and finally the determinant of the matrix for each energy is evaluated. Once the list of energies has been exhausted, an inverse interpolation procedure is performed to determine the energy zeroes of the determinant. The programs have been constructed for fcc and bcc lattices of one atom per unit cell; A. C. Switendick of these laboratories has written IBM programs for the more complex NaCl structure.¹³

RESULTS OF COMPUTATIONS

The calculations reported here were performed using the potential listed in Table I; this potential is that which Manning¹⁴ and Greene and Manning¹⁵ used in their cellular calculations on iron. The valence electrons in metallic iron are the $3d$ and $4s$ electrons, the ground configuration of atomic iron being $3d^64s^2$. The choice of this potential was made partly to compare the APW and cellular calculations and partly because the potential was one which had been subjected¹⁷ to a form of self-consistency check. For details of the construction of this potential the reader is referred to Manning's paper. Essentially, the potential is derived from an argon core (from the calculation of Manning and

¹³ A. C. Switendick, Quarterly Progress Report, No. 40, Solid State and Molecular Theory Group, Massachusetts Institute of Technology, 1961 (unpublished).

¹⁴ M. F. Manning, Phys. Rev. **63**, 190 (1943).

¹⁵ J. B. Greene and M. F. Manning, Phys. Rev. **63**, 203 (1943).

TABLE II. Summary of lattice parameter values used in various calculations.

Manning bcc	5.40 a.u.
Stern bcc	5.404 a.u.
Suffczynski bcc	5.405 a.u.
Callaway bcc	not given
Wood bcc	5.406 a.u.
Manning and Greene fcc	6.86 a.u.
Wood fcc	6.892 a.u.
In the APW calculations reported here, the sphere radius R_s (see text) values were:	
bcc	2.341 a.u.
fcc	2.437 a.u.

Goldberg¹⁶) plus one $4s$ -type and six $3d$ -type valence electrons. The $3d$ charge was composed of a sum of 6 different radial distributions, each weighted to reflect the concentration of levels described by density-of-states curves for transition metals then available. Manning's criterion for self-consistency was that the width of the d band at the end of the cellular calculation check the width given by the previous approximation. This potential was derived from Manning's bcc calculation and was taken over directly for the Greene and Manning fcc cellular calculations, no modifications being made for the different structure and interatomic distance.

Comparison of the results reported here with those of Manning and Manning and Greene shows that the agreement is not good. Consequently, one might well argue that the self-consistency procedure of Manning (or some more elaborate method) should be carried to conclusion for the APW calculations. This has not been done although it does not appear that such a job is

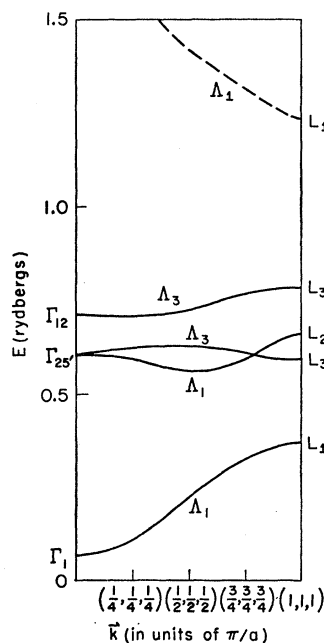


FIG. 2. Energy bands in fcc iron from $\Gamma(0,0,0)$ to $L(1,1,1)$ along $[111]$ direction.

¹⁶ M. F. Manning and L. Goldberg, Phys. Rev. **53**, 662 (1938).

TABLE III. Energies of states in fcc structure. All values are in rydberg units and are with reference to a zero constant potential between spheres. To convert energy levels so that they are with reference to the tabulated potential, subtract 0.776 ry from each. The symbols preceding the coordinates of the points refer to fcc Brillouin zone labels. The symbols preceding the energies are irreducible representation labels as defined by Bouckaert, Smoluchowski, and Wigner. The latter portion of the table lists some higher states which fall outside the first 6 bands.

4k	Band 1	Band 2	Band 3	Band 4	Band 5	Band 6
Γ 0,0,0	1 0.069	25' 0.606	25' 0.606	25' 0.606	12 0.712	12 0.712
Δ 0,2,0	1 0.125	2' 0.583	5 0.630	5 0.630	1 0.686	2 0.723
Δ 0,4,0	1 0.267	2' 0.516	1 0.639	5 0.692	5 0.692	2 0.748
Δ 0,6,0	1 0.356	2' 0.456	1 0.722	5 0.769	5 0.769	2 0.775
X 0,8,0	1 0.355	3 0.430	2 0.786	5 0.807	5 0.807	4' 0.871
Λ 1,1,1	1 0.112	1 0.594	3 0.622	3 0.622	3 0.709	3 0.709
Λ 2,2,2	1 0.225	1 0.563	3 0.624	3 0.624	3 0.722	3 0.722
Λ 3,3,3	1 0.342	1 0.590	3 0.609	3 0.609	3 0.769	3 0.769
L 4,4,4	1 0.371	3 0.595	3 0.595	2' 0.658	3 0.787	3 0.787
Σ $\frac{3}{2}, \frac{3}{2}, 0$	1 0.132	3 0.583	2 0.626	1 0.627	4 0.694	1 0.719
Σ $3, 3, 0$	1 0.295	3 0.543	1 0.603	4 0.667	2 0.673	1 0.795
Σ $\frac{9}{2}, \frac{9}{2}, 0$	1 0.451	1 0.520	3 0.546	4 0.670	2 0.733	1 0.958
K 6,6,0	1 0.421	1 0.468	3 0.618	4 0.721	2 0.780	3 1.168
W 4,8,0	2' 0.435	3 0.532	3 0.532	1 0.695	1' 0.808	3 1.299
Γ	15 2.491					
L	1 1.228					
W	1 1.527	2' 1.447				
X	1 1.445					
K	1 1.260	1 1.470				

insuperable with the digital computers now available. In addition to the potential, the specification of the problem requires a value of the lattice constant and a value of the sphere radius R_s . This information is given in Table II along with the values used by Stern,¹⁷ Callaway,¹⁸ Suffczynski,¹⁹ and Manning^{14,15} in their calculations.

The results of the calculations are listed in Tables III and IV and in Figs. 1 through 9. The \mathbf{k} points for which

bcc calculations were made were determined by a cubic grid in k space of dimensions $(\frac{1}{4} \times \frac{1}{4} \times \frac{1}{4})$. The fcc calculations were carried out for a lesser number of points. Our units for measurement of k are indicated in the tables.

The curves are drawn using the information given in the tables and the compatibility relations as outlined by Bouckaert, Smoluchowski, and Wigner.¹⁰ The labeling of the irreducible representations of the wave functions associated with the various $E(\mathbf{k})$ is that of these authors. It is, of course, possible to draw many more such curves, using the information in the tables; we have presented the curves along the directions of high symmetry plus one bcc case (Fig. 9) in which we show the band structure along a line lying in the plane

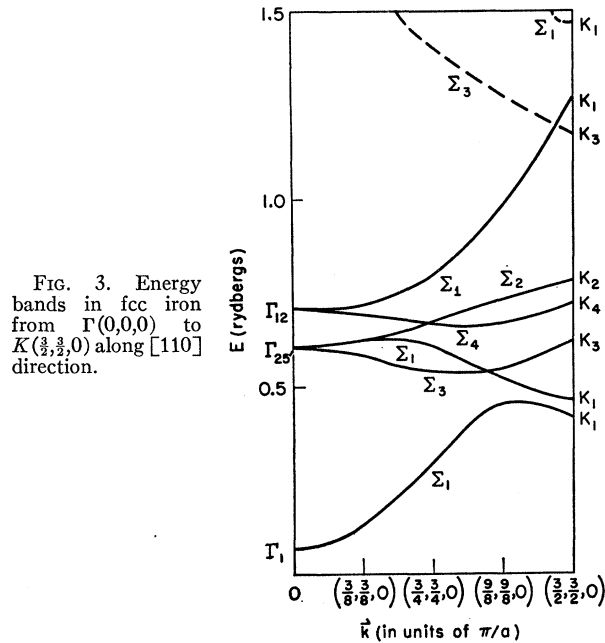


FIG. 3. Energy bands in fcc iron from $\Gamma(0,0,0)$ to $K(\frac{3}{2}, \frac{3}{2}, 0)$ along [110] direction.

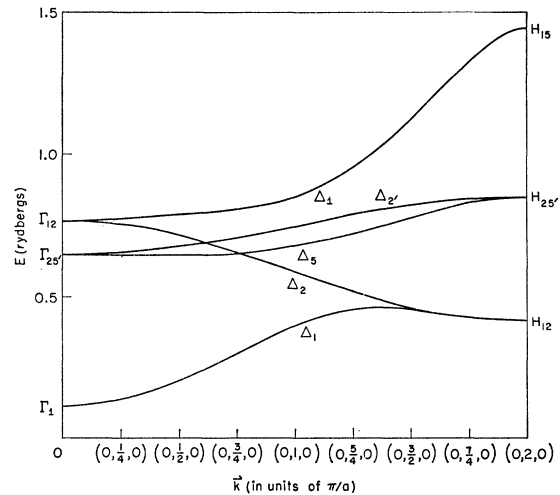


FIG. 4. Energy bands in bcc iron from $\Gamma(0,0,0)$ to $H(0,2,0)$ along [010] direction.

¹⁷ F. Stern, Phys. Rev. **116**, 1399 (1959).

¹⁸ J. Callaway, Phys. Rev. **99**, 500 (1955).

¹⁹ M. Suffczynski, Acta. Phys. Polon. **16**, 161 (1957).

TABLE IV. Energies of states in bcc structure. All values are in rydberg units and are with reference to a *zero* constant potential between spheres. To convert energy levels so that they are with reference to the tabulated potential, *subtract* 0.816 ry from each. The symbols preceding the coordinates of the points refer to bcc Brillouin zone labels. The symbols preceding the energies are irreducible representation labels as defined by Bouckaert, Smoluchowski, and Wigner. (A plus or minus sign indicates the behavior of the associated wave function upon reflection in the symmetry plane in which \mathbf{k} lies.) The latter portion of the table lists some higher states, which fall outside the first 6 bands.

4k	Band 1	Band 2	Band 3	Band 4	Band 5	Band 6
Γ 0,0,0	1 0.108	25' 0.640	25' 0.640	25' 0.640	12 0.762	12 0.762
Δ 0,1,0	1 0.132	5 0.644	5 0.644	2' 0.654	2 0.756	1 0.771
Δ 0,2,0	1 0.199	5 0.643	5 0.643	2' 0.676	2 0.716	1 0.786
Δ 0,3,0	1 0.297	2 0.650	5 0.651	5 0.651	2' 0.702	1 0.808
Δ 0,4,0	1 0.396	2 0.581	5 0.674	5 0.674	2' 0.741	1 0.849
Δ 0,5,0	1 0.450	2 0.517	5 0.715	5 0.715	2' 0.782	1 0.948
Δ 0,6,0	1 0.449	2 0.464	5 0.771	5 0.771	2' 0.817	1 1.118
Δ 0,7,0	1 0.424	2 0.425	5 0.824	5 0.824	2' 0.841	1 1.318
H 0,8,0	12 0.413	12 0.413	25' 0.850	25' 0.850	25' 0.850	15 1.435
Σ 1,1,0	1 0.154	2 0.631	1 0.642	3 0.676	1 0.757	4 0.773
1,2,0	+ 0.208	- 0.614	+ 0.627	- 0.700	+ 0.723	+ 0.777
1,3,0	+ 0.303	+ 0.612	- 0.616	+ 0.694	- 0.737	+ 0.800
1,4,0	+ 0.398	+ 0.570	- 0.634	+ 0.696	- 0.777	+ 0.847
1,5,0	+ 0.454	+ 0.515	- 0.672	+ 0.709	- 0.815	+ 0.961
1,6,0	+ 0.455	+ 0.468	- 0.725	+ 0.747	- 0.843	+ 1.142
G 1,7,0	1 0.442	4 0.439	3 0.788	1 0.804	2 0.861	4 1.332
Σ 2,2,0	1 0.275	2 0.594	1 0.618	3 0.751	1 0.753	4 0.773
2,3,0	+ 0.341	- 0.581	+ 0.608	+ 0.738	- 0.787	+ 0.789
2,4,0	+ 0.407	- 0.586	+ 0.592	+ 0.733	- 0.826	+ 0.850
2,5,0	+ 0.448	+ 0.551	- 0.616	+ 0.713	- 0.853	+ 0.988
G 2,6,0	1 0.467	4 0.507	3 0.669	1 0.722	2 0.867	4 1.143
Σ 3,3,0	1 0.383	2 0.560	1 0.656	1 0.767	4 0.784	3 0.835
3,4,0	+ 0.403	- 0.553	+ 0.667	+ 0.761	+ 0.833	- 0.861
G 3,5,0	1 0.429	3 0.579	4 0.618	1 0.737	2 0.874	4 0.947
N 4,4,0	1 0.399	2 0.545	1' 0.748	1 0.765	4 0.787	3 0.877
Λ 1,1,1	1 0.177	3 0.626	3 0.626	1 0.694	3 0.763	3 0.763
1,2,1	+ 0.229	+ 0.605	- 0.608	+ 0.727	- 0.731	+ 0.773
1,3,1	+ 0.320	- 0.590	+ 0.607	- 0.708	+ 0.767	+ 0.800
1,4,1	+ 0.410	- 0.557	+ 0.623	- 0.703	+ 0.790	+ 0.862
1,5,1	+ 0.466	- 0.513	+ 0.639	- 0.727	+ 0.813	+ 0.989
1,6,1	+ 0.469	- 0.473	+ 0.676	- 0.775	+ 0.832	+ 1.174
F 1,7,1	3 0.450	3 0.450	1 0.737	3 0.834	3 0.834	3 1.378
2,2,1	+ 0.286	- 0.582	+ 0.594	+ 0.748	- 0.767	+ 0.775
2,3,1	0.361	0.571	0.593	0.744	0.786	0.830
2,4,1	0.426	0.559	0.600	0.737	0.806	0.906
2,5,1	0.467	0.544	0.599	0.738	0.830	1.036
2,6,1	+ 0.477	- 0.507	+ 0.620	+ 0.754	- 0.835	- 1.187
3,3,1	+ 0.395	- 0.550	+ 0.620	+ 0.761	- 0.780	+ 0.876
3,4,1	0.418	0.549	0.645	0.761	0.801	0.936
3,5,1	+ 0.441	+ 0.563	- 0.605	+ 0.744	- 0.605	- 1.018
D 4,4,1	1 0.418	4 0.544	3 0.694	1 0.774	2 0.788	3 0.951
Λ 2,2,2	1 0.350	3 0.570	3 0.570	3 0.767	3 0.767	1 0.834
2,3,2	+ 0.409	- 0.551	+ 0.564	- 0.756	+ 0.781	+ 0.893
2,4,2	+ 0.458	- 0.537	+ 0.583	- 0.751	+ 0.792	+ 0.979
2,5,2	+ 0.500	- 0.527	+ 0.573	- 0.760	+ 0.800	+ 1.118
F 2,6,2	3 0.520	3 0.520	1 0.567	3 0.794	3 0.794	3 1.294
3,3,2	+ 0.451	- 0.539	+ 0.568	+ 0.767	- 0.780	+ 0.963
3,4,2	0.467	0.538	0.597	0.771	0.792	1.047
3,5,2	+ 0.482	+ 0.542	- 0.581	+ 0.765	- 0.794	- 1.139
D 4,4,2	1 0.465	4 0.537	3 0.625	1 0.780	2 0.790	3 1.083
Λ 3,3,3	1 0.518	3 0.538	3 0.538	3 0.785	3 0.785	1 1.057
3,4,3	+ 0.506	- 0.535	+ 0.562	- 0.780	+ 0.785	+ 1.154
F 3,5,3	1 0.508	3 0.556	3 0.556	3 0.787	3 0.787	3 1.282
D 4,4,3	1 0.517	4 0.535	3 0.574	1 0.788	2 0.793	3 1.232
P 4,4,4	4 0.541	4 0.541	4 0.541	3 0.791	3 0.791	4 1.393
Γ	15 3.09					
H	12 1.91	1 2.25				
P	1 1.53					
N	1 1.34	4' 1.97				

ΓPH , which line has only the symmetry of the plane.

The hatches along the abscissa indicate the points at which calculations were performed. The figures of

the respective Brillouin zones may be found in many places; in particular, see reference 3, p. 117.

It can be seen from the figures that the interaction of what are commonly referred to as s and d bands is

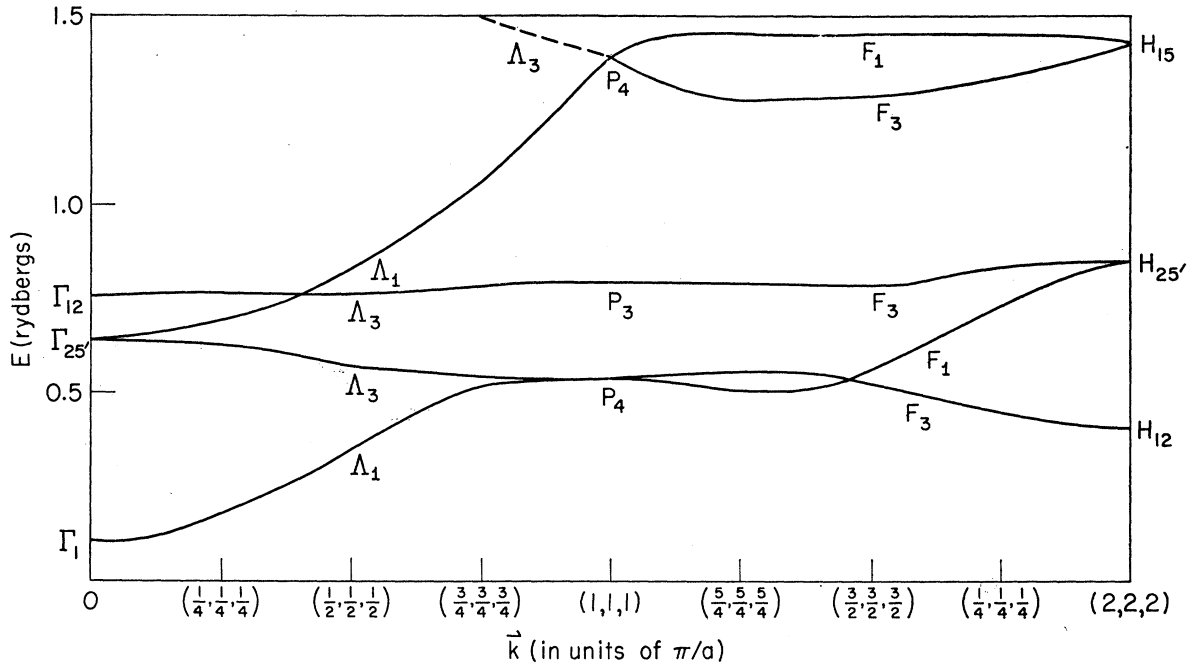


FIG. 5. Energy bands in bcc iron from $\Gamma(0,0,0)$ to $H(2,2,2)$ along $[111]$ direction.

taken automatically into account by virtue of using all angular momenta in the spherical expansion and all wave vectors allowed by Bloch's theorem in the plane-wave portion of the trial functions. Use of the appropriate projection operators ensures that the functions attached to the various $E(\mathbf{k})$ transform appropriately and include all proper combinations of the spherical harmonics. [For some irreducible representations of some \mathbf{k} , it is known²⁰ that certain angular momenta l cannot provide a basis; in these cases, the application of the projection operators results omission of terms of these l from the expressions (10).]

The dashed curves in the diagrams are sketched in by guesswork. They connect the higher energy levels at points of high symmetry for which calculations were performed—calculations at these higher energies have not yet been carried out for the points of lower symmetry so the dashed curves are only approximate.

The density-of-states curve for the bcc phase was compiled from the results of the calculations, which determine the energy at 1024 points in the complete Brillouin zone, weighting each point both according to degeneracy and symmetry. Figure 10 is a histogram constructed using steps $\Delta E=0.05$ ry. Figure 11 is a smooth curve chosen to fit two histograms constructed using $\Delta E=0.02$ ry; only the d band is shown here. Figure 12 indicates the number of states per atom which are available at any energy and again we assumed each state is doubly occupied. No density-of-states curve has been calculated for the fcc structure because of the

comparatively small number of points at which calculations were performed. More extensive calculations for the fcc case were not performed because the potential used was determined by Manning for the bcc case only; this potential was merely inserted into the fcc structure with no changes to take account of the

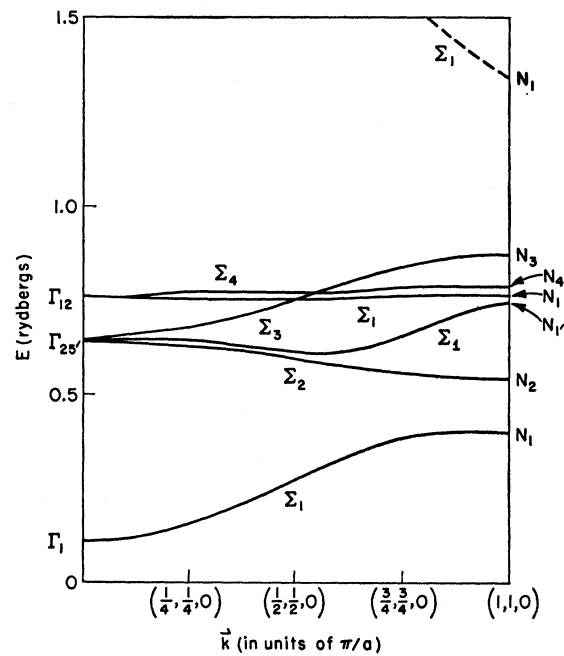


FIG. 6. Energy bands in bcc iron from $\Gamma(0,0,0)$ to $N(1,1,0)$ along $[110]$ direction.

²⁰ D. G. Bell, *Revs. Modern Phys.* 26, 106 (1954).

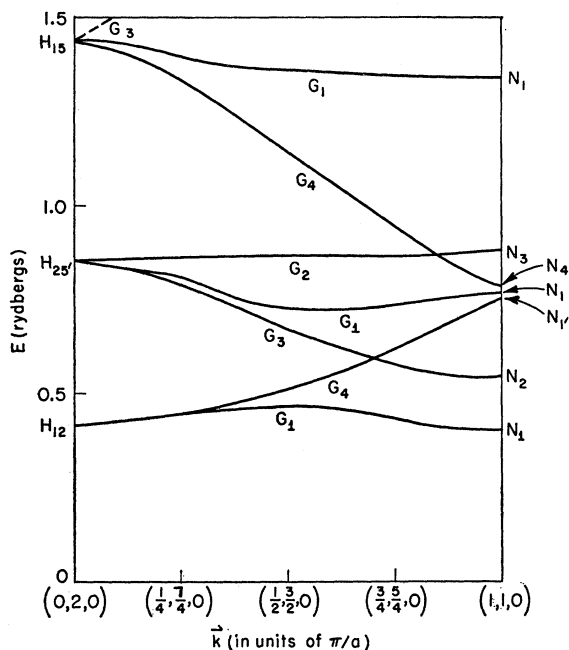


FIG. 7. Energy bands in bcc iron from $H(0,2,0)$ to $N(1,1,0)$ along line $k_x + k_y = 2$.

change in lattice constant and number of nearest neighbors. For these reasons and in view of limited computer availability, we felt the bulk of effort should go into elucidating the bcc case.

The location of the Fermi level ($E_F = 0.770$ ry) as defined here is obtained by filling each available state with one electron of each spin and thus might be re-

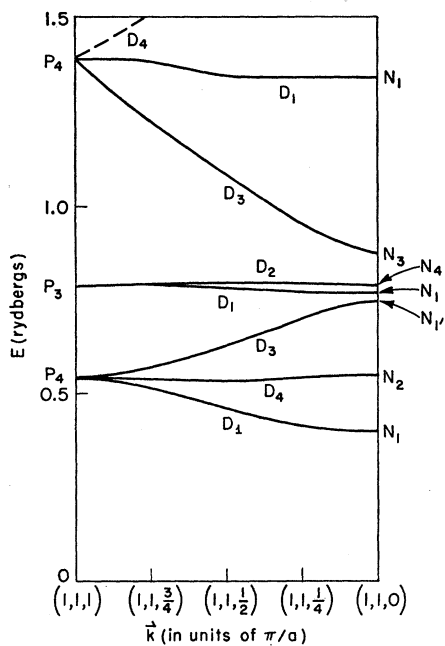


FIG. 8. Energy bands in bcc iron from $P(1,1,1)$ to $N(1,1,0)$ along line $k_x = k_y = 1$.

ferred to as a "nonmagnetic" Fermi level. If we call the energy location corresponding to H_{12} the bottom of the d band, then the *occupied* width of this band is 0.36 ry or 4.9 ev.

This density-of-states curve is qualitatively similar to the curves previously deduced for the transition series metals. The general features of the curve agree with those in Belding's publication²¹ although the extent of the curve along the energy axis is roughly double that of hers. In both curves one observes the familiar two principal maxima separated by a fairly deep minimum. However, this minimum does not dip down to zero and separate the band structure into two nonoverlapping regions of allowed energies; here, we are in agreement with the predictions of Callaway's investigations²² of d bands in cubic lattices. While we do not have a density-of-states curve for the fcc case,

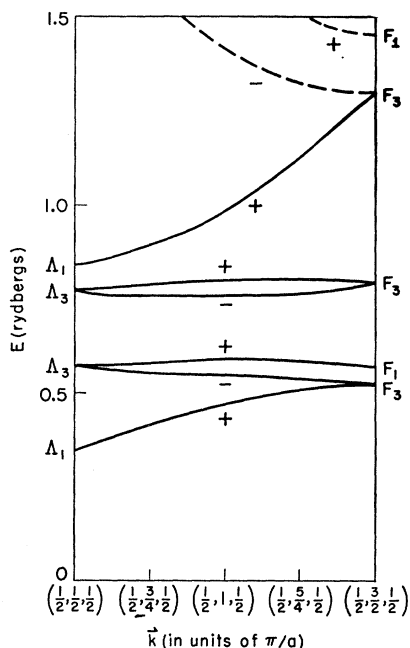


FIG. 9. Energy bands in bcc iron from $\Lambda(\frac{1}{2}, \frac{1}{2}, \frac{1}{2})$ to $F(\frac{1}{2}, \frac{3}{2}, \frac{1}{2})$ along a line in the $k_x = k_y$ plane. This indicates how one may map out the behavior of $E(\mathbf{k})$ throughout the zone, using the information in Table IV.

it is clear from the $E(\mathbf{k})$ curves for this structure that again no separation is obtained.

Cheng, Wei, and Beck²³ have calculated, from their measurements of electronic specific heats of transition metal alloys, a density-of-states curve for the transition series assuming a rigid band model. Our curve is in qualitative disagreement with theirs; they obtain an extremely high value of the density of states to the left

²¹ Ellinor F. Belding, *Phil. Mag.* **4**, 1145 (1959).

²² J. Callaway, *Phys. Rev.* **115**, 386 (1959); **120**, 731 (1960); **121**, 1351 (1961).

²³ C. H. Cheng, C. T. Wei, and P. A. Beck, *Phys. Rev.* **120**, 426 (1960).

of the iron peak, somewhere between Cr and Mn, which we do not find at all. This may be due to a breakdown of the rigid band model and thus it would be useful to have a series of calculations for the transition metals to test this hypothesis.

If we take our density-of-states curve and arbitrarily promote a total charge per atom of one electron of down spin from below $E=0.77=E_F$ and move it up into the unoccupied region above, thus giving us 2 Bohr magnetons per atom to account for the saturation magnetization, then we find that the Fermi level for spin-down electrons is located at $E=0.69$ ry [at which $N(E)$ is 0.77 electron/atom/ev] and that for spin-up electrons is located at $E=0.83$ ry [at which $N(E)$ is 1.68 electrons/atom/ev]. These two Fermi levels must match, of course, which means we should slide the density-of-states curve for up spin 0.14 ry to the left. Recalling that the curve as drawn is for *double* occupancy of each state, we see that we have at this new Fermi level $0.77/2+1.68/2=1.22$ electrons per atom

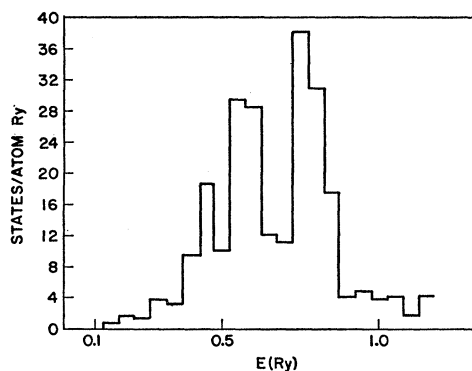


FIG. 10. Density-of-states curve for bcc iron. Histogram constructed using $\Delta E=0.05$ ry.

per ev. Cheng, Wei, and Beck give a value of about 2.0 electrons/atom ev. The bandwidth, defined in the sense used earlier, is now 0.42 ry or 5.7 ev for the spin-up electrons and 0.28 ry or 3.8 ev for spin-down electrons. The bandwidths as measured from the respective $E(\Gamma_1)$ are 9.8 ev and 7.9 ev, respectively. Tombouliau and Bedo²⁴ estimate, from the valence band emission spectra, that the bandwidth is 8.0 ev.

If this description of the magnetic state, in which we have identical density of states curves for each spin shifted away from one another (presumably by exchange interactions), is taken, then the new composite density-of-states curve for the d band that is obtained is sketched in Fig. 13. Comparing with the original case, we see that the major peak has been reduced in height, the minimum has been "sharpened" though not reduced and the left-hand peak has increased somewhat in height. While this description, in which we have arbitrarily lowered the energies of all spin-up electrons

²⁴D. H. Tombouliau and D. E. Bedo, Phys. Rev. **121**, 146 (1961).

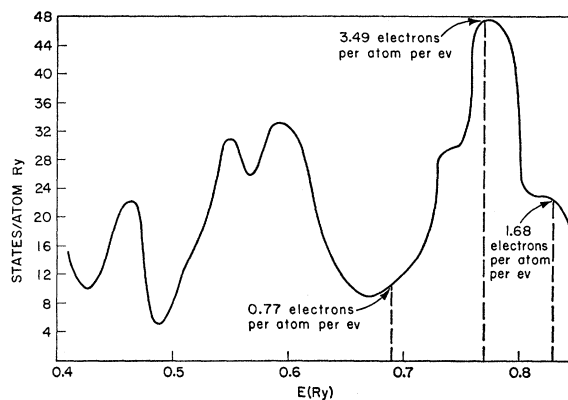


FIG. 11. Smoothed density of states for d band of bcc iron.

by the same 0.14 ry is oversimplified, it does seem likely that a band calculation in which the spin-up and spin-down electrons were handled separately might considerably change the structure of the conventional density-of-states curve.

A level-by-level comparison of the bcc calculation with other bcc iron calculations is given in Table V. One would not expect agreement among the calculations, since different potentials were used and various approximations were introduced. However, the agreement among the present results and those of Stern is much better than one might expect. Stern's value of the width of the occupied portion of the d band is 0.33 ry as compared with our value of 0.36 ry for the non-magnetic state. Stern's description of his density-of-states curve is one that agrees with ours.

It is reassuring that it is possible to use two quite different methods of solution of the energy band problem and yet obtain comparable results. It has been only in the last ten or fifteen years that we have been in a position to compare different calculations, simply because we can have confidence that each calculation represents an accurate solution of the problem pre-

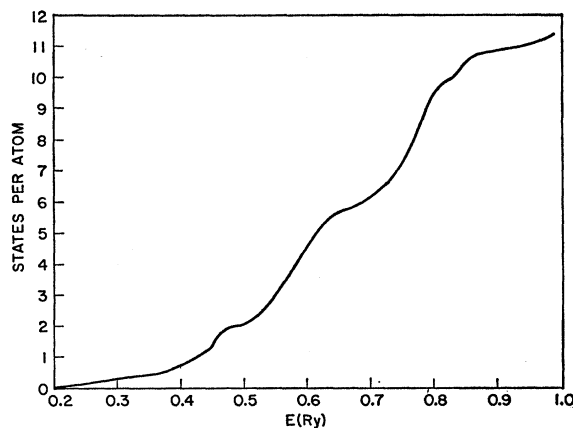


FIG. 12. Number of states per atom available at a given energy for bcc iron.

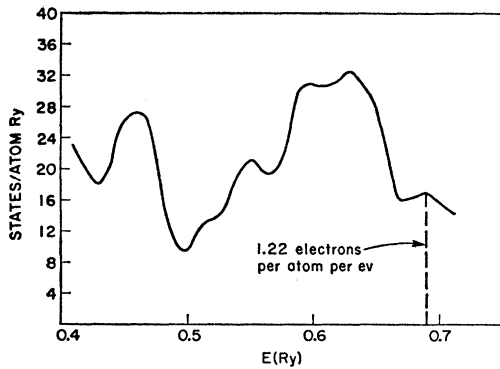


FIG. 13. Composite density-of-states curve for d band of bcc iron in which bands for spin-up electrons have been shifted 0.14 ry downward from those for spin-down electrons.

sented. These accurate solutions have been made possible through the great improvement of computing machines; it is no longer necessary to make drastic approximations in order to fit the problem to the machine.

We regard the energy levels quoted here as accurate to 0.003 ry. Table VI indicates the convergence of the levels in terms of the length of the largest wave vector entering the APW determinant. The general conclusion is that it is adequate to go out to fourth-nearest neighbors in reciprocal space for construction of the wave vectors $\mathbf{k} + \mathbf{K}_j$. Of course, for a point of no symmetry this implies a large (of the order of 40×40) secular equation but aside from computer time requirements, this imposes no difficulty.

Insofar as the cutoff on l goes, we have uniformly used all angular momentum up to $l=12$ in these calculations. Increasing this number up to $l=19$ affects the eigenvalues in the seventh decimal place. Examination of a few states at Γ indicates that cutting off at $l=8$ is perfectly satisfactory. However, in this method, it is necessary to include angular momenta beyond $l=2$ even though one normally speaks only of s , p , and d bands.

The possibility of extending up to high angular mo-

TABLE V. Comparison of bcc Fe energy band calculations. The energies are taken relative to the respective $E(H_{12})$ and are in rydberg units.^a

	Stern	Wood	Callaway	Suffczynski ^b	Manning
$\Gamma_{25'}$	+0.09	+0.23	+0.03	+0.08	-0.10
Γ_{12}	+0.32	+0.35	+0.05	+0.16	+0.00
H_{12}	0	0	0	0	0
$H_{25'}$	+0.58	+0.44	+0.07	+0.21	+0.52
P_4	+0.11	+0.13		+0.10	+0.04
P_2	+0.37	+0.38		+0.16	+0.38
N_1	-0.01	-0.01	-0.03	+0.04	-0.12
N_2	+0.02	+0.04	+0.03	+0.03	-0.10
N_3	+0.13	+0.35	+0.06	+0.16	+0.37
N_4	+0.37	+0.38	+0.08	+0.15	+0.38
N_5	+0.68	+0.47	+0.04	+0.21	+0.52
Over-all d band-width	0.68	0.47	0.12	0.21	0.62

^a Energies estimated from graphs in case of other authors.

^b Calculation in which second-nearest neighbors were used.

menta and large wave vectors in construction of the APW determinant with little difficulty is an extremely useful feature of the APW method. We need calculate only three l -dependent functions, viz., the Legendre polynomials, the spherical Bessel functions, and the logarithmic derivatives u_l'/u_l in the assumed potential, all of which are relatively easy to calculate. No complicated auxiliary functions are necessary in the method.

CONCLUSIONS

The APW method has proved to be a powerful method for solving the one-electron Schrödinger equation for a metal. It is not restricted to points of high symmetry in the Brillouin zone and thus it is possible to make a thorough investigation throughout the zone without the necessity of relying on interpolation procedures. There is no necessity for solving for the core-state wave functions²⁵ as in the orthogonalized plane-wave method. The method is one which is peculiarly adaptable to a digital computer so that the calculational burden is almost entirely removed.

A quite general question still remains to be answered, however, and that is the choice of the one-electron potential for a particular problem. In the framework of the energy-band method, this must be the self-consistent potential generated by the occupied one-electron Bloch functions. Most energy-band calculations, including the present one, assume that this potential is not greatly different from what one would obtain using atomic functions (perhaps somewhat modified) for these occupied one-electron functions. This assumption has worked moderately well, but now that we are in a position to obtain the actual Bloch functions from all \mathbf{k} it appears feasible to use these in a self-consistent field method. This would put us in an excellent position to assess the limits of the energy-band method.

TABLE VI. Energies of two sample bcc levels as a function of the square of the length of the wave vector of the last APW included in the secular equation. [In our units, the first-nearest neighbors in \mathbf{k} space are of the type (2,2,0).]

$ \mathbf{k} ^2$	E	$ \mathbf{k} ^2$	E	$ \mathbf{k} ^2$	E
Point $\mathbf{k} = (2,5,1)/4$					
13.9	0.7584	19.9	0.7394	26.9	0.7367
14.9	0.7554	20.9	0.7387	27.9	0.7356
15.9	0.7495	21.9	0.7386	28.9	0.7352
16.9	0.7407	23.9	0.7385	30.9	0.7351
17.9	0.7403	24.9	0.7382	31.9	0.7351
18.9	0.7396	25.9	0.7368	32.9	0.7351
Point $\mathbf{k} = (2,3,0)/4$; odd representation					
16.8	0.7994	26.8	0.7895	34.8	0.7880
17.8	0.7954	28.8	0.7889	36.8	0.7878
19.8	0.7913	29.8	0.7883	37.8	0.7878
20.8	0.7912	31.8	0.7881	38.8	0.7876
23.8	0.7907	32.8	0.7880	42.8	0.7876
25.8	0.7898				

²⁵ M. M. Saffren, Ph.D. Thesis, Department of Physics, Massachusetts Institute of Technology (1959) (unpublished).

The potential used in the present calculations has led to results which seem to be in fair agreement with experiment; calculation of more \mathbf{k} points and a consequent refinement of the density-of-states curves might be indicated, although we feel this is hardly worthwhile until we have a better potential. We have compared bandwidth and electronic specific heat and found reasonable agreement. The experimental controversy with regard to the number of $3d$ electrons in iron seems to have been satisfactorily resolved by recent experiments of Batterman *et al.*²⁶; it appears that no *qualitative* change of the conventional energy-band picture is necessary to explain the experimental results.

Perhaps one obvious feature of the calculations should be mentioned. These calculations, as well as Stern's, have produced a valence band whose occupied width is considerable; we cannot very well consider the d bands to be "narrow bands." This has come about because both in our calculations and in Stern's, the form of the radial d function has not been assumed *a priori* as atomic, but has in fact been calculated for the case under consideration and the changes have been considerable enough to widen the bands beyond what one might expect on the basis of a simple tight-binding argument.

In conclusion, we are now in a position to map out accurately the one-electron wave functions and energy levels throughout the entire Brillouin zone and thus it should be possible to answer quantitatively the questions as to what Fermi surfaces may look like, how the total electronic charge density behaves as a function of position, how much hyperfine interaction we might expect from an energy-band picture, etc. By and large, most of the past effort has been directed at the behavior of the one-electron energies but the previous questions are equally important ones.

Notes added in proof. Recent reports of calculations

²⁶ B. W. Batterman, D. R. Chipman, and J. J. DeMarco, Phys. Rev. **122**, 68 (1961).

on energy bands in copper carried out by Segall,²⁷ using the Chodorow potential, show excellent agreement with Burdick's calculations.⁹ Segall has used the Green's function method of Kohn and Rostocker, as described by Ham and Segall.²⁸ We, thus, have good cross checks among Chodorow's hand calculations,⁵ the calculations of Burdick, and the calculations of Segall.

Wohlfarth and Cornwell²⁹ have recently presented a density of states curve for bcc iron which exhibits sharp peaks which are known to be demanded.³⁰ Our curves do not show these peaks; the peaks have been smoothed out by the numerical methods used in constructing the curves. The presence of the peaks could be extremely important, as Wohlfarth and Cornwell point out, and may explain (among other things) the sharp peak observed by Cheng, Wei, and Beck.²³

ACKNOWLEDGMENTS

The writer thanks Professor J. C. Slater, who suggested the problem, for his continued interest and support. He is also indebted to members of the Solid-State and Molecular Theory Group at the Massachusetts Institute of Technology for many discussions. Especial thanks are due to M. M. Saffren for use of computer programs and for many discussions which were invaluable.

He also thanks the staff of the MIT Computation Center for advice, help, and use of the Whirlwind and IBM computation systems. A portion of the calculations was performed at the computing installation of the Lincoln Laboratory of the Massachusetts Institute of Technology and the writer is grateful for the extension of their facilities.

²⁷ B. Segall, Phys. Rev. Letters **7**, 154 (1961); Phys. Rev. **125**, 109 (1962).

²⁸ F. S. Ham and B. Segall, Phys. Rev. **124**, 1786 (1961).

²⁹ E. P. Wohlfarth and J. F. Cornwell, Phys. Rev. Letters **7**, 342 (1961).

³⁰ L. Van Hove, Phys. Rev. **89**, 1189 (1953); J. C. Phillips, Phys. Rev. **104**, 1263 (1956).